

Magnetic contributions to the low-temperature specific heat of the ferromagnetic insulator $\text{Pr}_{0.8}\text{Ca}_{0.2}\text{MnO}_3$

A. Wahl^a, V. Hardy, C. Martin, and Ch. Simon

Laboratoire CRISMAT^b, Institut des Sciences de la Matière et du Rayonnement – Université de Caen, 6 boulevard du Maréchal Juin, 14050 Caen Cedex, France

Received 21 May 2001 and Received in final form 14 December 2001

Abstract. The $\text{Pr}_{1-x}\text{Ca}_x\text{MnO}_3$ system exhibits a ferromagnetic insulating state for the composition range $x \leq 0.25$. A metallic ferromagnetic state is never realized because of the low hole concentration and the very small averaged A-site cation radius. In the present study, the nature of the magnetic excitations at low temperature has been investigated by specific heat measurements on a $\text{Pr}_{0.8}\text{Ca}_{0.2}\text{MnO}_3$ single crystal. The decrease of the specific heat under magnetic field is qualitatively consistent with a suppression of ferromagnetic spin waves in a magnetic field. However, at low temperature, the qualitative agreement with the ferromagnetic spin waves picture is poor. It appears that the large reduction of the specific heat due to the spin waves is compensated by a Schottky-like contribution possibly arising from a Zeeman splitting of the ground state multiplet of the Pr^{3+} ions.

PACS. 65.40.Ba Heat capacity – 75.50.-y Studies of specific magnetic materials – 75.30.Ds Spin waves

Hole-doped perovskite manganese oxides $\text{R}_{1-x}\text{AE}_x\text{MnO}_3$ (R and AE, being trivalent rare-earth and divalent ions, respectively) are associated with a wide variety of electronic and magnetic properties depending on the value of x and the averaged A-site cation radius, $\langle r_A \rangle$ [1]. These materials have recently been the subject of intense studies due to intriguing phenomena such as charge/orbital ordering (CO) [2] or colossal magnetoresistance (CMR) [3]. The latter is usually interpreted by means of the double-exchange interaction (DE) theory [4]. Although the DE mechanism cannot account alone for the temperature dependence of the resistivity – recent theoretical works have claimed that additional interactions, such as strong dynamical Jahn-Teller based electron-lattice coupling are necessary to explain the magnitude of the resistivity drop associated with the onset of ferromagnetism [5] – such a scenario gives an interesting qualitative interpretation of coupled ferromagnetic ordering and metallicity. Within such a framework, the ferromagnetic (FM) ordering is related to a large electronic itinerancy *i.e.* metallic behavior.

Among the hole-doped perovskite manganese oxides, the $\text{Pr}_{1-x}\text{Ca}_x\text{MnO}_3$ system (PCMO) is of great interest [6–12]. For $0.3 \leq x < 0.8$, charge ordering of Mn^{3+} and Mn^{4+} (CO) is found and an antiferromagnetic (AFM) ordering can be observed with Néel temperature ranging from 100 K to 170 K for $x = 0.8$ and 0.3, respectively. A metallic state is never realized under zero field for this composition range except upon application of pres-

sure [13], light [14], high current [15] and magnetic field. For $x \leq 0.25$, a ferromagnetic insulator (FMI) state is always observed. Indeed, a ferromagnetic metallic state (FMM) can never be realized because of the low hole concentration and the small averaged A-site cation radius, $\langle r_A \rangle$ [10–12, 16–19] which result in a decrease of the magnitude of W and, consequently, in a reduction of the effectiveness of the DE interaction, mostly responsible for the absence of the FMM state.

We have performed a calorimetric study of the FMI $\text{Pr}_{0.8}\text{Ca}_{0.2}\text{MnO}_3$. The aim of this paper is to answer to the following question: What is the nature of the magnetic contribution in the FMI state? We expect the analysis of the low temperature specific heat data (C) to provide accurate values of lattice, electronic and magnetic components in the FM state. According to both insulating and ferromagnetic behaviors reported for this compound, one might expect the determination of the relevant contributions to C to be rather simple. However, as often reported in the literature, we have found that an analysis based on a single set of zero field data cannot yield unambiguous results. Thus, investigation of the magnetic field induced specific heat change appears to be an essential tool.

In this paper, we focus on the reduction of the specific heat under magnetic field. In order to shed further light on whether this reduction of specific heat can be totally ascribed to a FMSW term, we have collected and analysed specific heat data in different magnetic fields. There is a clear decrease of the signal that is consistent with a suppression of the FMSW in a magnetic field. Through a scaling approach, a quantitative agreement is found with the

^a e-mail: alexandre.wahl@ismra.fr

^b Unité Mixte de Recherches 6508

FMSW theory for high temperature whereas the agreement is poor at lower temperature. Besides, a modelling of the temperature and field dependence of the low temperature magnetization within the sole FMSW picture is also mainly unsuccessful. To fully describe the low temperature specific heat, we suggest that an additional Schottky-like contribution might be considered. Finally, the change of specific heat under magnetic field has finally been modelled by a large reduction of specific heat due to FMSW that is compensated by an increase in C due to Zeeman splitting of the Pr^{3+} ions.

Using the floating-zone method with a feeding rod of nominal composition $\text{Pr}_{0.8}\text{Ca}_{0.2}\text{MnO}_3$, a several-cm-long single crystal was grown in a mirror furnace. Two samples were cut out of the central part of this crystal, one of them for resistivity measurements and the other for magnetization and specific heat measurements. X-ray diffraction and electron diffraction studies, which were performed on pieces coming from the same part of the crystal, attested that the samples are single phased, and well crystallized. The cell is orthorhombic with a Pnma space group, in agreement with previously reported structural data. The energy dispersive spectroscopy analyses confirm that the composition is homogeneous and close to the nominal one, in the limit of the accuracy of the technique. The electron diffraction characterization was also carried out *versus* temperature, from room temperature to 92 K. The reconstruction of the reciprocal space showed that the cell parameters and symmetry remain unchanged in the whole domain of temperature and, more especially, no extra reflections have been detected. This electron diffraction observation, coupled with lattice imaging, shows that, in our sample there is no charge ordering effect, even at short range distances. All X-ray and electron diffraction observations agree with previous published results for compounds of the same system [20].

Specific heat measurements were carried out by using the two- τ relaxation method, at temperatures from 2.2 to 300 K and under magnetic fields up to 9 T. The background signal, including the exact amount of Apiezon N used to paste the sample on the platform, was recorded in a first run, and it was then subtracted from the total heat capacity. The absence of any significant field dependence of this background signal was carefully checked in the low temperature range (2.2–15 K).

Resistivity measurements were performed by the standard four-probes technique, at temperatures from 5 to 300 K, and fields up to 9 T. Magnetization measurements were recorded by using a superconducting quantum interference device magnetometer, at temperatures from 5 to 300 K, and fields limited to 5 T. The ac susceptibility was measured in zero dc field with an alternating field $hac = 1$ Oe for various frequencies.

The temperature dependence of the specific heat (C), the ac susceptibility (χ) and the resistivity (ρ), up to 300 K and under zero field, are shown in Figure 1 for our $\text{Pr}_{0.8}\text{Ca}_{0.2}\text{MnO}_3$ crystal. The data are shown up to high temperature to characterize the overall behaviour of this compound. In all the measurements, the tem-

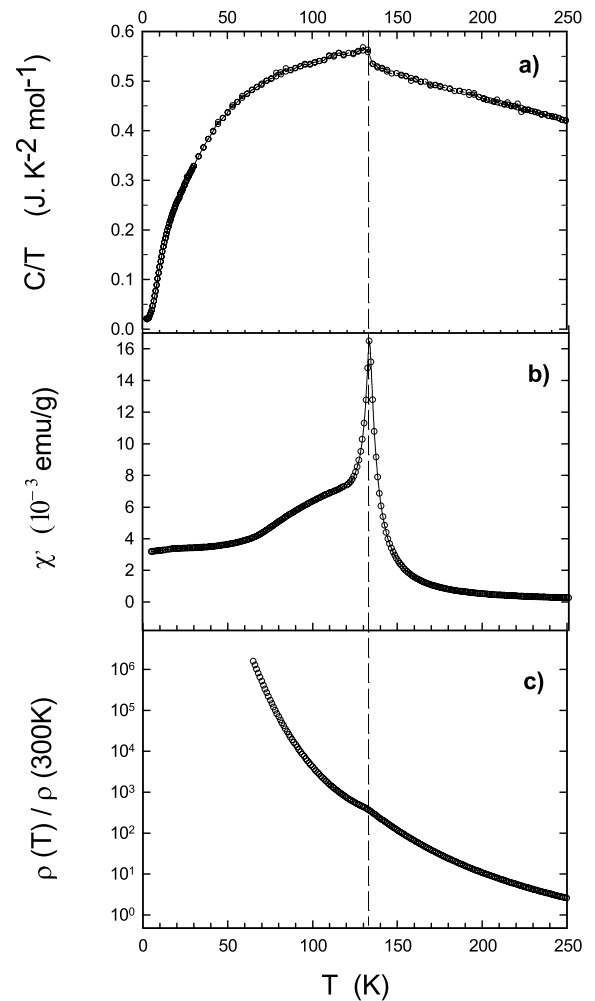


Fig. 1. Temperature dependence of (a) the specific heat divided by temperature C/T under zero field; (b) the real part of ac susceptibility χ' ($hac = 1$ Oe; 1000 Hz); (c) the normalized resistivity under zero field.

perature dependence is dominated by a salient feature at the paramagnetic-ferromagnetic (PM-FM) transition, $T_c \sim 135$ K. The transition in C/T *vs.* T , corresponding to the onset of the FM ordering, is evidenced as a sharp asymmetric anomaly (Fig. 1a). Figure 1b shows the temperature dependence of the real part of the susceptibility, χ' ($hac = 1$ Oe, 1000 Hz). The rise in $\chi'(T)$ at a temperature around 135 K, associated with the onset of the FM ordering is followed, on lowering the temperature, by a broad shoulder. One observes a continuous decrease of $\chi'(T)$ down to 50 K where a trend to saturation occurs. The zero field temperature dependence of the resistivity (Fig. 1c) does not show any temperature-induced I-M transition. However, a slight change in the slope takes place at the same temperature as the other features described above. Isothermal M *vs.* H curve measured at 5 K (Fig. 2), shows that magnetization first increases up to 2.5 tesla where the saturation value ($4.3 \mu_B/\text{f.u.}$) is reached. This is higher than the expected magnetic moment from Mn spins contributions taking into account the relative concentration

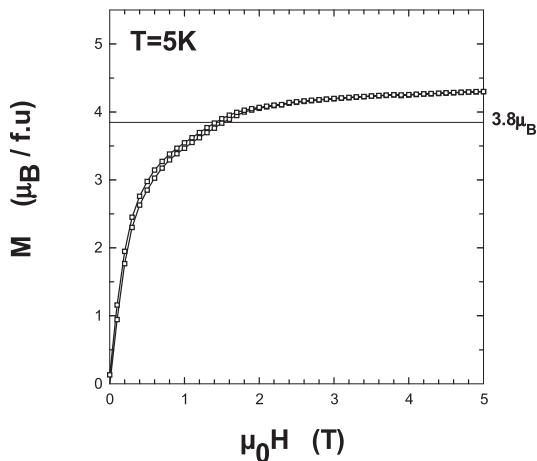


Fig. 2. Field dependence of the magnetization at 5 K.

of Mn^{3+} and Mn^{4+} in the compound ($3.8 \mu_{\text{B}}/\text{f.u.}$). This feature is often reported in the PCMO systems and is generally attributed to an additional ferromagnetic moment arising from the FM ordering of the Pr spins with respect to the Mn spins [14,21].

As a first step, we examine how informations concerning the relevant contributions to C can be extracted from zero field data. In this paper, we confine the analysis to the data above 4 K for which the hyperfine term, related to splitting induced by large local magnetic fields at the Pr and Mn nuclear spins, is assumed to be negligible. Various contributions are usually considered for the specific heat in this low temperature range. First, a phononic term arising from lattice vibrations has to be included. At low temperature, *i.e.* $T \leq 10$ K, this contribution can fairly be approximated by a βT^3 term (a T^5 term may be added when an analysis is carried out up to higher temperature). Although no carriers contribution to C is expected for $\text{Pr}_{0.8}\text{Ca}_{0.2}\text{MnO}_3$ – this contribution has the form of a linear temperature term, γT , where γ is proportional to the density of states at the Fermi level – many insulator systems show the appearance of such a linear term in the specific heat due to spin disorder [6,22]. If the gap is assumed to be zero then the magnetic term associated with the FMSW excitations under zero field is $\delta T^{3/2}$ with $\delta = 0.113 R a^3 (\frac{k_{\text{B}}}{D})^{3/2}$ where a is the lattice parameter of the elementary perovskite cell and R , the ideal gas constant. The assumption of a zero spin gap is supported by numerous experimental evidences [23,25].

In this section, we have attempted to model the zero field low temperature data (4 K–10 K) assuming that the total specific heat might be comprised of the 3 above terms. The fitting procedure including the 3 terms all together does not converge at all if β , δ and γ are left as free parameters. This procedure yields unphysical values for δ and γ depending on the temperature range investigated; thus, as a first step, we have considered only the FMSW contribution ($\delta T^{3/2}$) beside the lattice term. Our result matches numerous reports where fitting using the $\delta T^{3/2}$ term makes a very small contribution to specific heat ($\delta = 2 \text{ mJ/K}^{5/2} \text{ mol}$) [6,8,23,24]. However, the ob-

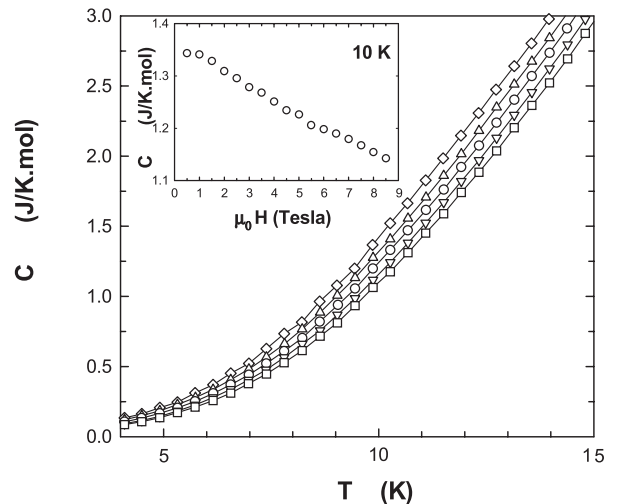


Fig. 3. C vs. T curves under various fields, recorded in the FCW mode [0 T (\circ); 3 T (\square); 5 T (Δ); 7 T (∇); 9 T (\diamond)]. Inset displays specific heat values at 10 K as a function of the magnetic field.

servation of a magnetic contribution to the specific heat of the FM phase of the doped manganite has generated conflicting results and the question of whether a set of zero field data is sufficient to observe a magnetic contribution was often raised.

A fitting of equally good quality can be obtained if one includes a sole linear term beside the lattice contribution. As pointed out above, including such a linear contribution is not senseless in our ferromagnetic insulator. Nevertheless, the linear coefficient γ is found to be $4 \text{ mJ/K}^2 \text{ mol}$ and such a small value is not consistent with values usually associated with spin disorder [6,22]. It must be pointed out that, in both cases, the fittings are achieved with β_3 parameters significantly larger than those usually associated with lattice contributions in hole-doped manganites ($\theta_{\text{D}} < 250$ K). However, although a softening of the lattice in the insulating phase has already been reported in many papers [8,26–28], this can not explain this very low Debye temperature.

As reported in previous work [8,21–24,26,27], we were unable to obtain reliable results concerning a FMSW contribution and/or a linear term characterizing the disorder using a standard fitting procedure for zero field data. Indeed, it is obvious that the present low temperature specific heat measurements without field cannot allow us to determine a unique set of values for the contributions presumably involved in the analysis. Thus, we expect the study of the change of specific heat under magnetic field to shed light on the nature of the contributions that occur at low temperatures.

The curves for 0, 3, 5, 7 and 9 tesla are shown in Figure 3. These data were registered upon warming the sample which was previously cooled under field (FCW mode). Measurements were also carried out with cooling under zero field (ZFC mode) and no significant change was observed. A decrease of the specific heat is observed under magnetic field; this feature is more obvious in the inset

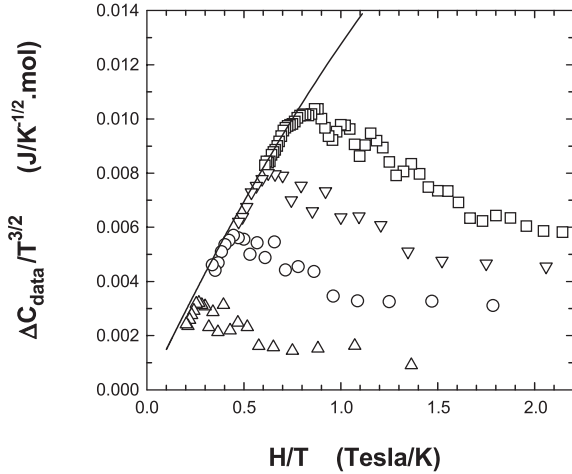


Fig. 4. $\frac{\Delta C_{\text{data}}}{T^{3/2}}$ vs. $\frac{H}{T}$ for different temperatures and fields. The solid line is the theoretical scaling function $G\left(\frac{H}{T}\right)$ given in the text. Several symbols stand for the quantities under different magnetic fields.

of Figure 3 where the field dependence of the specific heat is directly measured at 10 K after zero field cooling. Such a decrease of the specific heat under magnetic field is at first sight consistent with thermodynamic expectations for a ferromagnet ($\frac{\partial C}{\partial H} < 0$). The results obtained for $\text{Pr}_{0.8}\text{Ca}_{0.2}\text{MnO}_3$ are in *qualitative* agreement with the suppression of the thermal excitations of the FMSW in the presence of a field induced gap. However, it is essential to check if the specific heat decrease under magnetic field is in *quantitative* agreement with the FMSW theory.

Under magnetic field, in the FM state, the magnetic term is expressed in the following way:

$$C_{\text{FMSW}}(H, T) = Ra^3 \left(\frac{k_B T}{D} \right)^{3/2} F \left(\frac{H}{T} \right)$$

where

$$F \left(\frac{H}{T} \right) = \frac{1}{4\pi^2} \int_{\frac{g\mu_B H}{k_B T}}^{\infty} \frac{x^2 e^x}{(e^x - 1)^2} \sqrt{x - \frac{g\mu_B H}{k_B T}} dx. \quad (1)$$

In this expression, the FMSW excitation at zero field is assumed to show no gap and $F(0) = 0.113$.

Hence, $\Delta C_{\text{FMSW}} = C_{\text{FMSW}}(0, T) - C_{\text{FMSW}}(H, T)$ is written in the form:

$$\begin{aligned} \Delta C_{\text{FMSW}} &= 0.113 Ra^3 \left(\frac{k_B T}{D} \right)^{3/2} \\ &\quad - Ra^3 \left(\frac{k_B T}{D} \right)^{3/2} F \left(\frac{H}{T} \right) = T^{3/2} G \left(\frac{H}{T} \right) \end{aligned} \quad (2)$$

with

$$G \left(\frac{H}{T} \right) = Ra^3 \left(\frac{k_B}{D} \right)^{3/2} \left[0.113 - F \left(\frac{H}{T} \right) \right]. \quad (3)$$

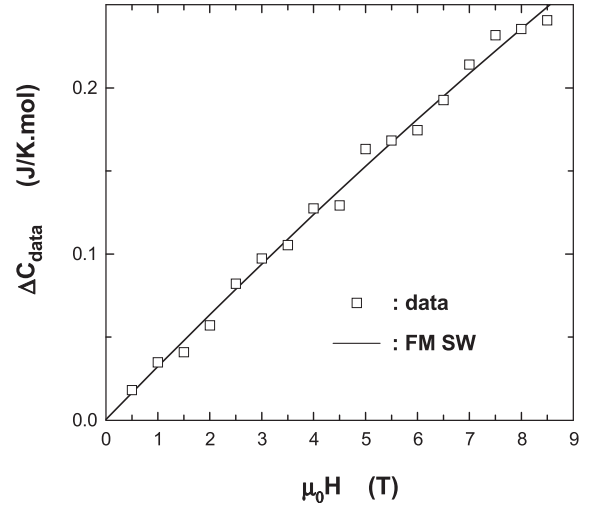


Fig. 5. $\Delta C_{\text{data}} = C_{\text{data}}(0, T) - C_{\text{data}}(H, T)$ at 13 K as a function of magnetic field. The solid line is the calculated FMSW contribution.

To avoid any experimental problem arising from the choice of a fitting procedure, the scaling approach seems to be the most promising way to emphasize the FMSW contribution. According to the above expression, $\frac{\Delta C_{\text{FMSW}}}{T^{3/2}}$ only depends on $\frac{H}{T}$; this could provide us a direct test for the reliability of the standard FMSW model. If all the magnetic specific heat arises from the field induced suppression of the FMSW, the plot $\frac{\Delta C_{\text{data}}}{T^{3/2}}$ vs. $\frac{H}{T}$ should show the same trend for data recorded for different temperatures and under various magnetic fields. Figure 4 illustrates that, at low temperature (highest values of $\frac{H}{T}$), $\Delta C_{\text{data}} = C_{\text{data}}(T, 0) - C_{\text{data}}(T, H)$ cannot be fully described by considering a magnetic contribution arising from the *sole* FMSW. However, while T is increased (for lower $\frac{H}{T}$ values), a superimposition of the data is observed suggesting that the description in term of FMSW becomes to be relevant. The solid line in Figure 4 corresponds to the calculated $G\left(\frac{H}{T}\right)$ scaling function considering $D \approx 15 \pm 3 \text{ meV \AA}^2$. Considering this latter value of the FMSW stiffness, the reduction of the specific heat as a function of the applied field is also compared to the prediction of the FMSW theory in Figure 5 for a temperature of 13 K ($0 \leq \frac{H}{T} \leq 0.69$). The value of the FMSW stiffness might seem very small compared to the ones derived through neutron scattering experiments for other manganites [29–31]. However, as emphasized by Roy *et al.* [21], the very soft SW in $\text{Pr}_{0.8}\text{Ca}_{0.2}\text{MnO}_3$ appears to be a general feature of the low doped region of the PCMO. These authors invoke a drastic effect of the ferromagnetic moment associated with the Pr ions.

Before going further, a modelling of the H - and T -dependence of the magnetization within the FMSW framework could support the above observation. The “Bloch $T^{3/2}$ law”, in which the presence of the field has been properly taken into account using the standard FMSW picture, has been tested. According to the procedure proposed by Smolyaninova *et al.* [32], the low

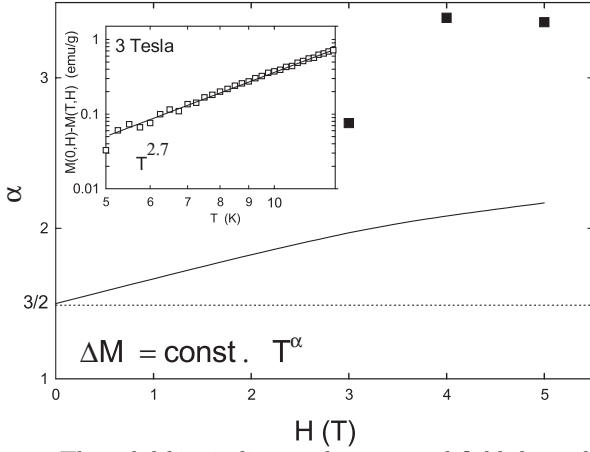


Fig. 6. The solid line indicates the expected field dependence of the exponent within the FMSW picture. The black squares are from data. Inset: Magnetization *vs.* temperature for $H = 3$ T. The line is the best fit to the power law (see text).

temperature magnetization follows the form:

$$M(0, H) - M(T, H) = (\text{const.}) \times T^\alpha \quad (4)$$

where $M(0, H)$ is the extrapolation of $M(T, H)$ back to $T = 0$. $M(0, H)$ for fields 3, 4 and 5 tesla agrees with the saturation value ($\approx 4.3\mu_B/\text{f.u.}$) derived from isothermal M *vs.* H measured at 5 K. The power law fits rather well the measured low temperature magnetization (within the range 5 K–15 K) with $\alpha = 2.7, 3.4$ and 3.35 for 3, 4 and 5 tesla, respectively. Using the standard SW picture, the magnetization per unit volume at low temperature is given:

$$M(0, H) - M(T, H) = g\mu_B \left(\frac{k_B T}{4\pi D} \right)^{3/2} \times f_{3/2} [g\mu_B (H - NM) / k_B T] \quad (5)$$

where $f_p(y) = \sum_{n=1}^{\infty} e^{-ny} / n^p$ and NM is the demagnetization field (0.4 tesla). Over the investigated range of temperature, the above relation can be well approximated by a power law (see inset Fig. 6). In Figure 6, the field dependence of α expected from the FMSW picture is compared to the values derived from the data. As seen in Figure 6, there exists a large discrepancy which indicates that the low temperature magnetization does not show the behavior expected for a simple spin wave picture.

Let us now turn back to the specific heat data. As shown before, for the very low temperature range, the change in the specific heat does not follow the temperature and magnetic field dependences of the *sole* FMSW. Indeed, it is obvious that the magnitude of the ΔC_{data} is not important enough to be described in such a way: there exists in the very low temperature range an excess of specific heat under magnetic field. Hence, we speculate that other contributions could also change under magnetic field. Using the calculated contribution of the FMSW at low temperature, we can obtain the field and temperature

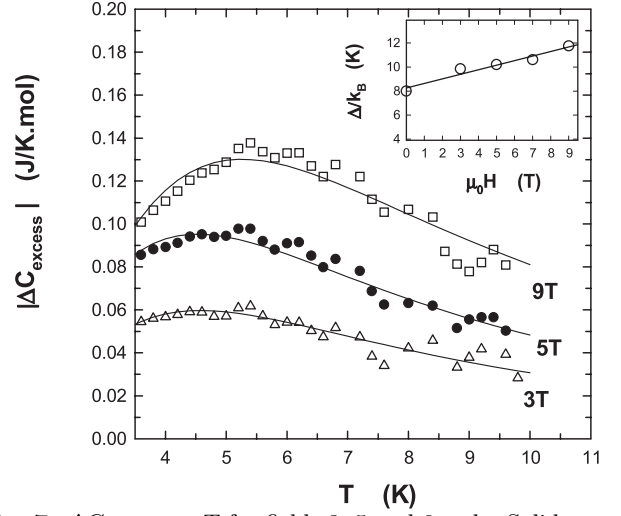


Fig. 7. ΔC_{excess} *vs.* T for fields 3, 5 and 9 tesla. Solid curves: fits to a two-level Schottky function. The inset shows the resulting energy splitting as a function of the applied magnetic field.

dependence of this excess specific heat:

$$\Delta C_{\text{excess}} = \Delta C_{\text{data}} - \Delta C_{\text{FMSW}}. \quad (6)$$

Results are illustrated in Figure 7. Bell-shaped curves are obtained with maxima slightly shifted to higher temperature as the field increases; the magnitude of the excess specific heat is also observed to increase with increasing fields. Such a behavior has a Schottky-like appearance and we speculate that this magnetic Schottky anomaly occurs due to the Zeeman splitting of the crystal field ground state multiplet of the Pr^{3+} ions [33] under magnetic field. Clearly, a true two-level system exists for spin $\frac{1}{2}$ ions only; for spins $J \neq \frac{1}{2}$, specific heat should be generalized to the multilevel Schottky function on the basis of the Langevin theory. However, a simplified two-levels system, where the effective moment of the Pr^{3+} in the ground state is μ and Δ , the size of the two levels system, should be a rather good approximation for the observed effect in specific heat. Δ is expressed in the form: $\Delta = 2\mu (H_{\text{int}} + H)$ where H_{int} is the internal field at the Pr^{3+} site and H , the applied magnetic field.

Hence, we have fitted the data (ΔC_{excess}) to a two-level Schottky function:

$$\Delta C_{\text{Sch}}(T, H) = C_{\text{Sch}}(T, H) - C_{\text{Sch}}(T, H = 0) \quad (7)$$

where

$$C_{\text{Sch}}(T, H) = n_{\text{Sch}} R \left(\frac{\Delta}{k_B T} \right)^2 \frac{\exp(\Delta/k_B T)}{(1 + \exp(\Delta/k_B T))^2} \quad (8)$$

where n_{Sch} is a coefficient taking into account the number of Schottky centers and the levels degeneracy. Fits for 3, 5 and 9 tesla, shown as solid curves in Figure 7, are in rather good agreement with the experimental data. The resulting energy splitting (inset Fig. 7) give $H_{\text{int}} = 22$ tesla and correspond to a magnetic moment of approximately $0.3\mu_B$. This value is similar to $0.5\mu_B$, estimated at low

temperature from magnetization measurements and neutron scattering experiments [14] and $0.8\mu_B$ from high field magnetization [34]. Thus, the large reduction of specific heat under magnetic field is partially compensated by a Schottky-like contribution arising from the ground state level splitting of the rare earth element. The level splitting derived from the specific heat data is in rough agreement with the one estimated from high field magnetization in $\text{Pr}_{0.7}\text{Ca}_{0.3}\text{MnO}_3$ (5 K for $H = 6$ T) [34].

The fact that the temperature dependence of the magnetization does not follow the prediction of the FMSW theory may be linked to the occurrence of a Schottky term in the specific heat measurements. Moreover, knowing the excess and spin wave contribution it is then possible to determine the phonon background which can be used as a reliable test for our description. This yields a Debye temperature $\theta_D \sim 325$ K which is typical of values already reported for the PCMO system [8].

There have already been reports of specific heat data in related materials in which Schottky like anomalies due to Zeeman splitting of the rare earth state is clearly seen. However, we address here the subtle role of two interacting spin systems (Pr and Mn ones) on the low temperature specific heat of a hole doped manganite. We speculate that the effect is the following: the Pr moments experience an effective molecular field produced by the Mn moments (H_{int}) and a concomitant modification of the specific heat (ΔC_{excess}) is obtained due to the molecular field induced splitting of the crystal field ground state multiplet of the Pr^{3+} .

In conclusion, low temperature specific heat measurements have been carried out on the ferromagnetic insulator $\text{Pr}_{0.8}\text{Ca}_{0.2}\text{MnO}_3$. Measurements of the specific heat under magnetic field have allowed us to obtain reliable informations on the nature of the magnetic excitations involved in the low temperature thermodynamic of $\text{Pr}_{0.8}\text{Ca}_{0.2}\text{MnO}_3$. We have shown that an analysis in terms of ferromagnetic spin waves is not sufficient for describing the entire magnetic contribution to specific heat. An additional contribution of Schottky-like nature, probably arising from the interaction of the Mn and Pr spin systems has to be included.

References

1. For a review, see *Colossal Magnetoresistance, Charge Ordering and Related Properties of Manganese Oxides*, edited by CNR. Rao, B. Raveau (World Scientific, Singapore, 1998) and *Colossal Magnetoresistive Oxides*, edited by Y. Tokura (Gordon and Breach Science, New York).
2. E.O. Wollan, W.C. Koehler, Phys. Rev. **100**, 545 (1955); J.B. Goodenough, *ibid.* **100**, 564 (1955).
3. S. Jin, T.H. Tiefel, M. McCormack, R.A. Fastnacht, R. Ramesh, L.H. Chen, Science **264**, 413 (1994); R. von Helmolt, J. Wecker, B. Holzappel, L. Schultz, K. Samwer, Phys. Rev. Lett. **71**, 2331 (1993).
4. C. Zener, Phys. Rev. **82**, 403 (1951); P.W. Anderson, H. Hasegawa, *ibid.* **100**, 675 (1955); P.-G. de Gennes, *ibid.* **118**, 141 (1960).
5. A.J. Millis, P.B. Littlewood, B.I. Shairman, Phys. Rev. Lett. **74**, 5144 (1995).
6. V.N. Smolyaninova, A. Biswas, X. Zhang, K.H. Kim, B.-G. Kim, S.-W. Cheong, R.L. Greene, Phys. Rev. B **62**, R6093 (2000).
7. M.R. Lees, J. Barratt, G. Balakrishnan, D. McK. Paul, M. Yethiraj, Phys. Rev. B **52**, R14 303 (1995).
8. M.R. Lees, O.A. Petrenko, G. Balakrishnan, D. McK. Paul, Phys. Rev. B **59**, 1298 (1999).
9. Y. Tomioka, A. Asamitsu, H. Kuwahara, Y. Morimoto, Y. Tokura, Phys. Rev. B **53**, R1689 (1996).
10. C. Martin, A. Maignan, M. Hervieu, B. Raveau, Phys. Rev. B **60**, 12 191 (1999).
11. A. Maignan, C. Martin, F. Damay, B. Raveau, Z. Phys. B **104**, 21 (1997).
12. Z. Jiráková, S. Krupička, Z. Šimša, M. Dlouhá, S. Vratilav, J. Magn. Magn. Mater. **53**, 153 (1985).
13. Y. Moritomo, H. Kuwahara, Y. Tomioka, Y. Tokura, Phys. Rev. B **55**, 7549 (1997).
14. D.E. Cox, P.G. Radaelli, M. Marezio, S.-W. Cheong, Phys. Rev. B **57**, 3305 (1998).
15. A. Asamitsu *et al.*, Nature **388**, 50 (1997).
16. F. Damay, C. Martin, A. Maignan, B. Raveau, J. Appl. Phys. **82**, 6181 (1997).
17. L.M. Rodriguez-Martinez, J.P. Attfield, Phys. Rev. B **54**, R15622 (1996).
18. O.A. Yassin, S.N. Bathia, I.H. Hagemusa, Solid State Commun. **116**, 207 (2000).
19. H.Y. Hwang, S.W. Cheong, P.G. Radaelli, M. Marezio, B. Batlogg, Phys. Rev. Lett. **75**, 914 (1995).
20. M. Hervieu, A. Barnabé, C. Martin, A. Maigan, B. Raveau, Phys. Rev. B **60**, R726 (1999).
21. M. Roy, J.F. Mitchell, A.P. Ramirez, P. Schiffer, Phys. Rev. B **62**, 13876 (2000).
22. L. Ghivelder, I. Abrego Castillo, M.A. Gusmao, J.A. Alonso, L.F. Cohen, Phys. Rev. B **60**, 12184 (1999).
23. J.J. Hamilton, E.L. Keatley, H.L. Ju, A.K. Raychaudhuri, V.N. Smolyaninova, R.L. Greene, Phys. Rev. B **54**, 14 926 (1996).
24. L. Ghivelder, I. Abrego Castillo, N. McN. Alford, G.J. Tomka, P.C. Riedi, J. MacManus-Driscoll, A.K.M. Akther Hossain, L.F. Cohen, J. Magn. Magn. Mater. **189**, 274 (1998).
25. S. Lofland *et al.*, Phys. Lett. A **209**, 246 (1995).
26. B.F. Woodfield, M.L. Wilson, J.M. Byers, Phys. Rev. Lett. **78**, 3201 (1997).
27. T. Okuda, Y. Tomioka, A. Asamitsu, Y. Tokura, Phys. Rev. B **61**, 8009 (2000).
28. T. Okuda, Y. Tomioka, A. Asamitsu, T. Kimura, Y. Taguchi, Y. Tokura, Phys. Rev. Lett. **81**, 3203 (1998).
29. J.W. Lynn, R.W. Erwin, J.A. Borchers, Q. Huang, A. Santoro, J.L. Peng, Z.Y. Li, Phys. Rev. Lett. **76**, 4046 (1996).
30. J.W. Lynn, R.W. Erwin, J.A. Borchers, Q. Huang, A. Santoro, J.L. Peng, R.L. Green, J. Appl. Phys. **81**, 5488 (1997).
31. Y. Endoh, K. Hirota, J. Phys. Soc. Jpn **66**, 2264 (1997).
32. V.N. Smolyaninova, J.J. Hamilton, R.L. Green, Y.M. Mukovskii, S.G. Karabashev, A.M. Balbashov, Phys. Rev. B **55**, 5640 (1997).
33. S. Rosenkranz, M. Medarle, F. Fauth, J. Mesot, M. Zolliker, A. Furrer, U. Staub, P. Lacorre, R. Osborn, R.S. Eccleston, V. Trounov, Phys. Rev. B **60**, 14857 (1999).
34. R.M. Thomas, V. Skumryev, J.M.D. Coey, S. Wirth, J. Applied Phys. **85**, 5384 (1999).